Global metallicity of globular cluster stars from colour-magnitude diagrams

F. Caputo¹ and S. Cassisi^{2,3}

- ¹ INAF-Osservatorio Astronomico di Roma, via di Frascati 33, 00040 Monte Porzio Catone, Italy caputo@coma.mporzio.astro.it
- ² INAF-Osservatorio Astronomico di Teramo, via M. Maggini, 64100 Teramo, Italy cassisi@te.astro.it
- ³ Max-Planck fur Astrophysik, Karl-Schwarzschild-Strasse 1, 85741 Garching, Germany

ABSTRACT

We have developed an homogeneous evolutionary scenario for H- and He-burning low-mass stars by computing updated stellar models for a wide metallicity and age range $(0.0002 \le Z \le 0.004)$ and $9 \le t(Gyr) \le 15$, respectively) suitable to study globular clusters. This theoretical scenario allows us to provide self-consistent predictions about the dependence of selected observational features of the colour-magnitude diagram, such as the brightness of the Turn Off (TO), Zero Age Horizontal Branch (ZAHB) and Red Giant Branch bump (BUMP), on the cluster metallicity and age.

Taking into account these predictions, we introduce a new observable based on the visual magnitude difference between the TO and the ZAHB [$\Delta M_V(\text{TO-ZAHB})$], and the TO and the RGB-bump [$\Delta M_V(\text{TO-BUMP})$], given by $A = \Delta M_V(\text{TO-BUMP}) - 0.566\Delta M_V(\text{TO-ZAHB})$. We show that the parameter A does not depend at all on the cluster age, whereas it does strongly depend on the cluster global metallicity. The calibration of the parameter A as a function of Z is then provided, as based on our evolutionary models. We tested the reliability of this result by also considering stellar models computed by other authors, employing different input physics. Eventually, we present clear evidence that the variation of $\Delta M_V(\text{TO-BUMP})$ with $\Delta M_V(\text{TO-ZAHB})$ does supply a powerful probe of the global metal abundance, at least when homogeneous theoretical frameworks are adopted. Specifically, we show that the extensive set of models by VandenBerg et al. (2000) suggests a slightly different calibration of A versus Z calibration, which however provides global metallicities higher by only 0.08 ± 0.06 dex with respect to the results from our computations.

We provide an estimate of the global metallicity of 36 globular clusters in the Milky Way, based on our A-Z calibration, and a large observational database of Galactic globular clusters. By considering the empirical [Fe/H] scales by both Zinn & West (1984) and Carretta & Gratton (1997), we are able to provide an estimate of the α -element enhancement for all clusters in our sample. We show that the trend of $[\alpha/\text{Fe}]$ with respect to the iron content significantly depends on the adopted empirical [Fe/H] scale, with the Zinn & West (1984) one suggesting α -element enhancements in fine agreement with current spectroscopical measurements.

Key words: globular clusters: metallicity – globular clusters: age – stars: evolution

1 INTRODUCTION

The colour-magnitude diagrams (CMDs) of globular clusters (GCs) present several features to be compared with the various constraints provided by stellar evolution theory. For this reason, they are often used to infer fundamental properties of ancient stellar populations and, in turn, of the early Universe.

It has been known for a long time that the absolute magnitude of the main-sequence turnoff (TO) can be calibrated in terms of the cluster age (t, in Gyr) and chemical composition parameters (Y, helium content) and Z, global metallicity. In order to overcome the uncertainties of obtaining accurate GC distances, it is common to use the difference in magnitude between the TO and the zero-age-horizontal-branch (ZAHB) at the RR Lyrae instability strip $(\log T_e \sim 3.85)$, whose luminosity level depends on Y and Z, with a negligible dependence on T. Besides this vertical method to get the cluster age, there is the so-called horizontal method, which is based on the determination of the TO

colour relative to some fixed point on the red giant branch (RGB – see Stetson, Vandenberg & Bolte 1996). As a whole, both methods are affected by the empirical difficulties to get the precise position of the TO in the CMD, as well as by several still-open intrinsic uncertainties on the evolutionary models, most notably the dependence on Z of the ZAHB luminosity, for the vertical method, and the efficiency of superadiabatic convection in the outer layers (i.e., the mixing length calibration) for the horizontal method, (see Rosenberg et al. 1999, hereafter R99, for details and references).

The determination of Z for GC stars is by itself problematic. Under the classical assumption of scaled-solar metal distribution, where all of the abundance ratios of the various metals relative to iron have the solar value, the correlation between the global metallicity Z and the measured iron-to-hydrogen ratio [Fe/H] is given by the classical relation $\log Z = [Fe/H] - 1.70$. One should however consider that current empirical scales for [Fe/H] (e.g., Zinn & West 1984, Zinn 1985, Rutledge, Hesser & Stetson 1997, and Carretta & Gratton 1997) may differ by up to ~ 0.3 dex. In addition, it has to be noticed that the assumption of scaledsolar chemical compositions might be rather inadequate for Galactic GC stars which show a not negligible overabundance of the so-called α -elements (O, Ne, Mg, Si, Ar, Ca, and Ti) with respect to iron-peak elements ($[\alpha/\text{Fe}] \sim 0.3$, according to Carney 1996). It follows that the relationship between the measured [Fe/H] and the overall metallicity Zshould follow the relation

$$\log Z = [Fe/H] - 1.70 + \log(0.638f + 0.362) \tag{1}$$

where f is the enhancement factor of α -elements with respect to iron (Salaris et al. 1993) * .

The knowledge of the cluster age and global metallicity is fundamental for studying another important feature of CMDs, i.e. the luminosity level of the so-called RGB-bump. This is an intriguing feature of the RGB luminosity function which has been predicted for a long time, since the pioneering theoretical studies by Thomas (1967) and Iben (1968), but whose identification in GCs occurred years later (King et al. 1985). A first comparison (Fusi Pecci et al. 1990) of the observed difference in visual magnitude between RGB-bump and ZAHB level with theoretical models showed that the predicted dependence of $\Delta V({\rm ZAHB\textsc{-}BUMP})$ on metallicity was nicely reproduced, but the zero point of the observed relation was ~ 0.4 mag too faint.

An exhaustive investigation on the dependence of the parameter $\Delta V({\rm ZAHB\text{-}BUMP})$ on the physical inputs adopted in stellar computations has been performed by Cassisi & Salaris (1997, hereinafter CS97). In the same work, it was clearly shown that a fine agreement between theory and observations does exist when updated RGB stellar models and observational data for GCs with spectroscopic measurements of both iron and $\alpha-$ element abundances, are considered. More recently, the same result was obtained by Zoccali et al. (1999) and Ferraro et al. (1999, hereinafter F99) by using a much larger sample of Galactic GCs than CS97.

However, one has also to notice that Bergbusch & Vandenberg (2001) have recently found a discrepancy of the order of 0.25 mag, when comparing the $\Delta V({\rm ZAHB\text{-}BUMP})$ values provided by their models with the observational data for 4 GCs at various metallicities.

In reality, the RGB-bump luminosity is also dependent on the age of the stellar population $(\delta V(\text{BUMP})/\delta \log t \sim 1)$, while the above investigations do not take into account the age of individual GCs. It is well known the current debate whether the Galactic GCs formed all at the same time or there was a significantly protracted formation epoch. A recent analysis of an homogeneous photometric database containing 34 Galactic GCs (R99) shows that within the intermediate-metallicity clusters (-1.2 \leq [Fe/H] \leq -0.9) there is a clear evidence of age dispersion, with some clusters up to \sim 30% younger than the oldest ones. As an example, we consider the globular cluster NGC 362 for which F99 give $\Delta V(\text{ZAHB-BUMP})$ =0.10 mag±0.12 mag and a global metallicity \dagger [M/H]=-0.99.

From the relations given by these authors

$$M_{V,BUMP} = 0.75 + 0.99 \log t + 1.58 [M/H] + 0.26 [M/H]^2$$
 (2)

$$M_{V,ZAHB} = 1.00 + 0.35[M/H] + 0.05[M/H]^2$$
 (3)

one has that the agreement between theory and observations occurs for a cluster age of ${\sim}14.9$ Gyr, which is the value derived by R99 for the bulk of coeval GCs, using the Straniero et al. (1997) theoretical isochrones. However, R99 find that the actual age of NGC 362 is ${\sim}$ 11.5 Gyr, in which case one obtains a $\Delta V({\rm ZAHB\text{-}BUMP})$ value by 0.21 mag, namely ${\sim}0.1$ mag larger than the observed one.

It should be noticed that R99 adopts the [Fe/H] scale by Carretta & Gratton (1997), without any correction due to α -enhancement and, in order to interpret the observed difference $\Delta V(\text{TO-ZAHB})$, a linear relation for the absolute magnitude of the ZAHB as a function of the metal content $(M_{V,ZAHB}=0.18([\text{Fe/H}]+1.5)+0.65)$, instead of the quadratic relations used by F99 [see Eq. (3)] and CS97 $(M_{V,ZAHB}=1.13+0.39[\text{M/H}]+0.06[\text{M/H}]^2)$. In other words, the quoted extensive investigations on the RGB-bump luminosity and the age of Galactic GCs are not mutually consistent, since they use different metallicity scales and adopt, as theoretical values for the RGB-bump and TO luminosity, different calibrations of the ZAHB luminosity in terms of metallicity.

In order to make a complete and self-consistent study of these most prominent features in CMDs, we present in section 2 an homogeneous set of theoretical evolutionary results which predict the TO, RGB-bump and ZAHB luminosity for a wide range of ages ($9 \le t(Gyr) \le 15$) and metal abundances ($0.0002 \le Z \le 0.004$). In section 3 we introduce a new parameter A defined as $A = \Delta M_V(\text{TO-BUMP}) - 0.566\Delta M_V(\text{TO-ZAHB})$, and we show that this depends only on the global metallicity Z, being unaffected by age. In order to test this result, the evolutionary models computed by Salaris & Weiss (1997, 1998) and by Vandenberg et al. (2000) are also considered. We show that the former ones are in close agreement with our computations, whereas in the latter case some significant differences are present, leading to

^{*} It is worth recalling that this relation holds strictly only in case of the scaled-solar metal mixture by Ross & Aller (1976). The coefficients of this relation has to be slightly changed when accounting for different solar metal distributions. However, these changes are very small (see Yi et al. 2001).

[†] [M/H]=[Fe/H]+log(0.638f+0.362).

Table 1. Selected parameters from the evolutionary models.

				-
Z	Age(Gyrs)	$M_V(\mathrm{TO})$	$M_V(\mathrm{Bump})$	$M_V({ m ZAHB})$
0.0002	9	3.543	-0.394	0.443
0.0002	10	3.677	-0.339	0.439
0.0002	11	3.794	-0.288	0.436
0.0002	12	3.923	-0.241	0.433
0.0002	13	4.010	-0.199	0.430
0.0002	14	4.090	-0.161	0.427
0.0002	15	4.164	-0.127	0.425
0.0006	9	3.733	-0.016	0.533
0.0006	10	3.855	0.036	0.529
0.0006	11	3.945	0.080	0.526
0.0006	12	4.067	0.109	0.523
0.0006	13	4.178	0.152	0.520
0.0006	14	4.247	0.192	0.517
0.0006	15	4.312	0.227	0.515
0.001	9	3.817	0.158	0.563
0.001	10	3.926	0.218	0.560
0.001	11	4.023	0.253	0.557
0.001	12	4.184	0.290	0.555
0.001	13	4.256	0.318	0.552
0.001	14	4.323	0.370	0.550
0.001	13	4.256	0.318	0.552
0.001	14	4.323	0.370	0.550
0.001	15	4.386	0.425	0.548
0.002	9	3.982	0.525	0.584
0.002	10	4.083	0.571	0.581
0.002	11	4.209	0.610	0.578
0.002	12	4.284	0.642	0.576
0.002	13	4.362	0.691	0.574
0.002	14	4.429	0.739	0.572
0.002	15	4.491	0.770	0.570
0.003	9	4.066	0.753	0.665
0.003	10	4.157	0.778	0.663
0.003	11	4.239	0.848	0.660
0.003	12	4.357	0.890	0.658
0.003	13	4.425	0.912	0.656
0.003	14	4.464	0.933	0.654
0.003	15	4.571	0.952	0.652
0.004	9	4.023	0.902	0.714
0.004	10	4.165	0.961	0.711
0.004	11	4.241	1.014	0.709
0.004	12	4.354	1.067	0.707
0.004	13	4.414	1.102	0.704
0.004	14	4.501	1.128	0.703
0.004	15	4.562	1.135	0.701

a slightly different formulation of the $\Delta M_V(\text{TO-BUMP})$ versus $\Delta M_V(\text{TO-ZAHB})$ relationship. Nevertheless, the parameter $A{=}\Delta M_V(\text{TO-BUMP}){-}0.487\Delta M_V(\text{TO-ZAHB})$ inferred from the Vandenberg et al.'s (2000) computations is again strongly dependent on global metal abundance with no dependence on age.

On this basis, the TO, ZAHB and RGB-bump observations collected by F99 and R99 for a large sample of Galactic GCs are interpreted. The resulting global metal abundances are presented in section 4, together with some clues to the α -element enhancement with respect to iron in Galactic GCs. A summary is finally given in the last section.

2 THEORETICAL MODELS

In order to understand the observed properties of CMDs and RGB luminosity functions of GCs, we need an homogeneous

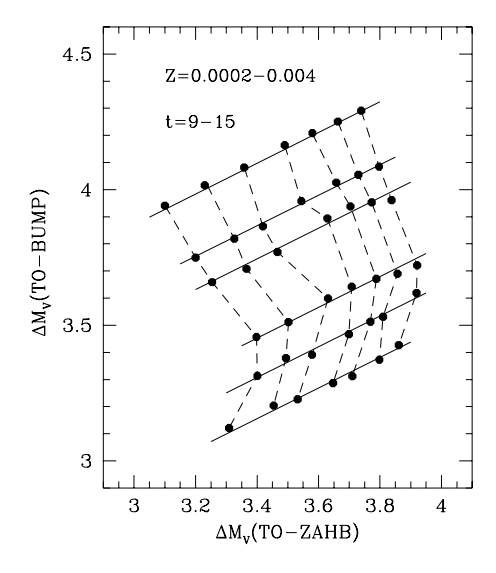
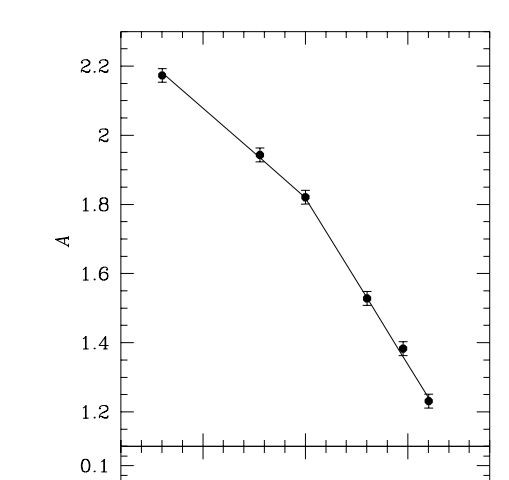


Figure 1. Theoretical predictions for $\Delta M_V(\text{TO-BUMP})$ and $\Delta M_V(\text{TO-ZAHB})$ as a function of age (t) and global metallicity (Z). The dashed lines refer to constant ages in the range of 9 to 15 Gyr (left to right), while the solid lines refer to constant metallicities in the range of 0.0002 to 0.004 (bottommost line). The solid lines have a similar slope of 0.566 (see text).

set of evolutionary models for both the H- and He-burning phases. In present work, we have adopted a set of theoretical models computed by using the FRANEC evolutionary code (Chieffi & Straniero 1989; CS97; Castellani et al. 1997). A subset of these stellar models and corresponding isochrones have been already presented by Cassisi et al. (1998, 1999). However, in order to improve the coverage of the wide metallicity range spanned by Galactic GCs, we have extended previous computations considering additional initial chemical compositions. The physical inputs adopted in the model computations have been already discussed by Cassisi et al. (1998). A short summary is given below.

We use the OPAL (Rogers et al. 1996) equation of state (EOS), supplemented, in the temperature-density regime not covered by the OPAL tables, by the EOS provided by Straniero (1988), plus a Saha EOS in the outer stellar layers. The radiative opacities provided by the OPAL group (Iglesias, Rogers & Wilson 1992) for temperatures larger than 10,000K are employed, together with the Alexander & Ferguson (1994) tables for lower temperatures. Electron conduction opacities come from Itoh et al. (1983). The boundaries of the convective regions are determined according to the canonical Schwarzschild criterion. Induced overshooting and semiconvection during the central He-burning phase have been accounted following the prescriptions given by Castellani et al. (1985). The standard mixing-length theory is used for evaluating the temperature gradient in the superadiabatic regions; the value of the mixing length param-



0.05

-0.1

-3.5

0 0.05

 $\log Z_{ev} - \log Z$

Figure 2. (top) - Mean value of the parameter $A=\Delta M_V$ (TO-BUMP) $-0.566\Delta M_V$ (TO-ZAHB) as a function of Z. The solid line is the analytic fit to the data (see Eq. (4) and Eq. (5) in the text). (bottom) - Difference between the evolutionary metallicity $\log Z_{ev}$ derived using Eq. (4) and Eq. (5) and the original value $\log Z$, as a function of $\log Z$. The discrepancy is within ± 0.03 dex (dashed line).

-2.5

-3

logZ

eter is fixed at 1.6 for all computations. This value allows to match the RGB effective temperatures of a selected sample of Galactic GCs provided by Frogel, Persson & Cohen (1983).

All the models include microscopic diffusion of both helium and heavy elements, using the formalism by Thoul et al. (1994). For a detailed discussion concerning the effects of atomic diffusion on both main-sequence stars and more evolved models, we refer the interested reader to Castellani et al. (1997) and Cassisi et al. (1998). It is well known that helioseismology provides clear evidence that helium and heavy element settling is occurring in the Sun (see Basu, Pinsonneault, & Bahcall 2000, and references therein). However, recent spectroscopic analyses of GC stars (Gratton et al. 2001; Castilho et al. 2000; Ramirez et al. 2001) show that the surface chemical patterns do not show the effects of atomic diffusion, at least for what heavy elements are concerned. This means that either chemical settling is less efficient in metal-poor stars, or some other physical mechanism at work in the stellar atmospheres counterbalances the effect of atomic diffusion. A firmer understanding of this topic has to wait for more accurate theoretical and observational investigations.

Evolutionary models with masses ranging from 0.6 to $1.3M_{\odot}$ have been computed from the Zero Age Main Sequence up to the tip of the RGB marking the triple-alpha ignition inside the degenerate He core. The explored range of

metallicity is $0.0002 \leq Z \leq 0.004$, while for each metallicity the same initial He abundance $Y{=}0.23$ has been adopted. The He-core mass M_c and the chemical stratification at the RGB He-flash provided by the different evolutionary models have been used to compute the ZAHB structures needed to estimate the ZAHB luminosity level at $\log T_e{=}3.85$, the average effective temperature of the RR Lyrae instability strip. Isochrones have been then constructed in the age range 9 - 15 Gyr.

Finally, all the models and isochrones have been transposed from the theoretical H-R plane to the observational (V,B-V) plane by using the bolometric corrections and colour-temperature relations provided by Castelli, Gratton & Kurucz (1997a,b). In Table 1, for the different chemical compositions adopted in present work, we report the TO, RGB-bump and ZAHB absolute visual magnitude, as a function of age.

3 THEORETICAL CALIBRATIONS

The data listed in Table 1 show that, at a fixed age, TO, RGB-bump and ZAHB luminosities decrease with increasing the metal content. At a fixed metallicity the TO and RGB-bump become fainter for larger ages, whereas the ZAHB level becomes slightly brighter, due to the slight increase of the He-core mass M_c with decreasing total mass of the progenitor on the RGB.

Figure 1 displays the two differential parameters ΔM_V (TO-ZAHB) and ΔM_V (TO-BUMP), as derived from the results in Table 1. The dashed lines show the theoretical trend at a constant age, in steps of 1 Gyr, from 9 Gyr (left) to 15 Gyr (right), while the solid lines refer to a constant Z from 0.0002 to 0.004 (bottommost line). The difference ΔM_V (TO-BUMP) increases for larger ages, at fixed Z, and decreases for larger metallicities, at fixed t. As for the parameter ΔM_V (TO-ZAHB), it increases with increasing Z up to $\log Z \sim -2.7$, and then it decreases for larger metallicities, at least when $Z \leq 0.004$. On this subject, we recall that all our models are computed with an initial helium abundance Y=0.23. Within the quoted range of metal content, the expected He increase due to an helium-to-heavy element enrichment ratio $\Delta Y/\Delta Z \sim 2.5$ is only $\Delta Y=0.01$, whereas for metallicities larger than Z=0.004 the original amount of helium is expected to become significantly larger. Furthermore, also the amount of extra-helium brought to the stellar surface by the first dredge up is expected to increase when moving towards larger metallicities. As a consequence, the above theoretical trends cannot be applied to very metal-rich clusters ($[Fe/H] \ge -0.6$).

The data in Fig. 1 disclose that, for ages between 9 and 15 Gyr, the variation of $\Delta M_V(\text{TO-BUMP})$ with $\Delta M_V(\text{TO-ZAHB})$ has a constant slope of 0.566 (solid lines), with the zero-point depending on Z. From the results listed in Table 1 we calculate then the mean value of the parameter $A=\Delta M_V(\text{TO-BUMP})-0.566\Delta M_V(\text{TO-ZAHB})$ for each given Z. The upper diagram in Fig. 2 shows that the results are well approximated by the following linear relations:

$$\log Z = +0.518 - 1.933A \tag{4}$$

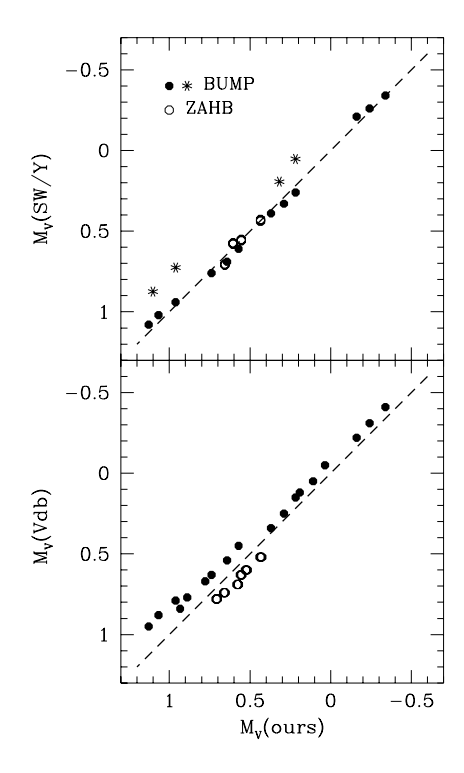


Figure 3. (top) - Comparison between our theoretical predictions for the RGB Bump and ZAHB luminosity and the ones provided by Salaris & Weiss (1997, 1998: open and filled circles, respectively) and Yi et al. (2001: asterisks). Each point corresponds to a fixed age and metallicity, for the values in common with our models. bottom) - As top panel, but for the models by Vandenberg et al. (2000). Open circles refer to the ZAHB luminosity, while full circles correspond to the RGB Bump luminosity.

$$\log Z = -1.110 - 1.039A \tag{5}$$

with $A \geq 1.82$ and A < 1.82, respectively. As it is shown in the lower panel of Fig. 2, the discrepancy between the *evolutionary* estimate of the global metallicity (hereafter Z_{ev}) based on the two differential parameters $\Delta M_V(\text{TO-BUMP})$ and $\Delta M_V(\text{TO-ZAHB})$, and the original value, is close to ± 0.03 dex.

Before proceeding further, it is worthwhile to compare our evolutionary predictions with similar computations provided by different authors. We considered the recent isochrones and ZAHB models computed by Salaris & Weiss (1997, 1998, hereinafter SW) and by Vandenberg et al. (2000, hereinafter Vdb, see also Bergbusch & Vandenberg 2001) with Z ranging from 0.0002 to 0.004 and ages in the range of 10-14 Gyr and 10-16 Gyr, respectively. We wish to notice that both sets of models do not account for atomic diffusion and have been computed by adopting a slightly different $\Delta Y/\Delta Z$ ratio (3 and 2, respectively). Moreover, they are computed under different assumptions about the α -element enhancement. In our comparison we used the Vdb models based on a scaled-solar heavy element distribution.

As shown in the upper panel of Fig. 3, both the ZAHB (open circles) and RGB-bump (filled circles) absolute magnitudes inferred from SW models are in close agreement with our results, whereas the Vdb computations plotted

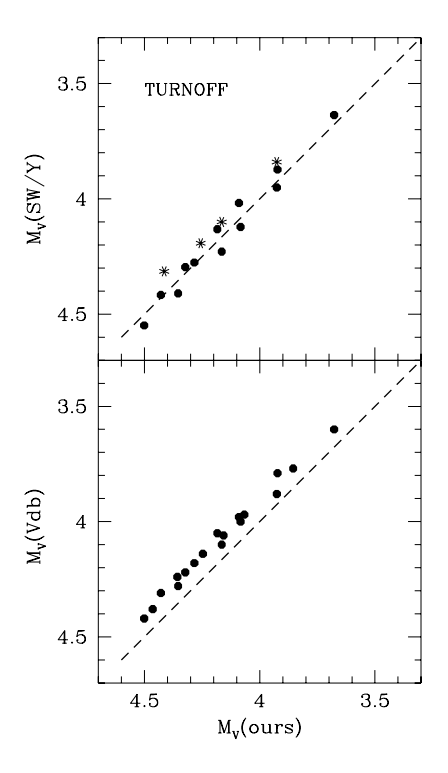


Figure 4. As in Fig. 3, but for the TO luminosity.

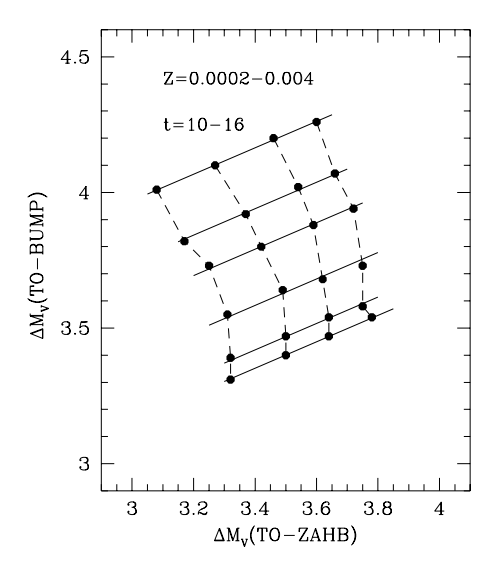


Figure 5. As in Fig. 1, but in this case the Vdb models have been adopted.

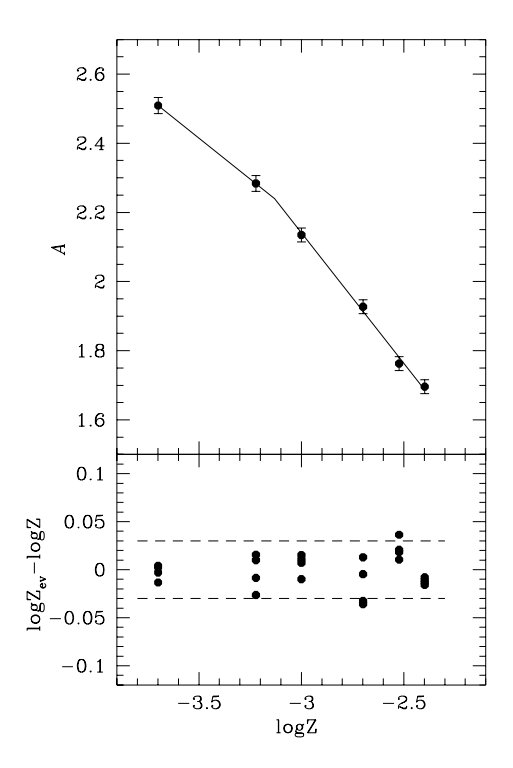


Figure 6. As in Fig. 2, but adopting the Vdb models.

in the lower panel suggest brighter RGB-bump and fainter ZAHB luminosities, with respect to the data in Table 1. The upper panel of Fig. 3 shows also the comparison between the RGB-bump absolute magnitudes provided by the recent Yale isochrones (Yi et al. 2001) and our results (asterisks), for the common values of metallicity (Z=0.001 and 0.004) and age (10 and 13 Gyrs). As a whole, one has that the Yale isochrones suggest brighter RGB-bumps than our models. Note that we were unable to carry out a similar comparison with the Yale ZAHB absolute visual magnitudes, as no data have been provided in the literature. Figure 4 deals with the TO luminosity provided by the quoted sets of computations, compared with the results in Table 1. We get that SW models are again in agreement with our predictions, whereas VdB and Yale models give brighter absolute magnitudes.

On the basis of the above discussion, we have considered the models by VdB for testing the effect of different input physics on the scenario suggested by our computations. Figure 5 presents $\Delta M_V(\text{TO-BUMP})$ versus $\Delta M_V(\text{TO-ZAHB})$, as derived from Vdb models. The dashed lines show the theoretical trend at a constant age, in steps of 2 Gyr, from 10 Gyr (left) to 16 Gyr (right), while the solid lines refer to a constant Z from 0.0002 to 0.004 (bottommost line). The general trend in Fig. 1 is here confirmed, but the variation of $\Delta M_V(\text{TO-BUMP})$ with $\Delta M_V(\text{TO-ZAHB})$ has a slope of 0.487 (solid lines). The correlation between the mean value of the parameter $A{=}\Delta M_V(\text{TO-BUMP}){-}0.487\Delta M_V(\text{TO-ZAHB})$ and $\log Z$ is presented in the upper diagram of Fig. 6, where the solid line depicts the relations

$$\log Z = +1.617 - 2.119A \tag{6}$$

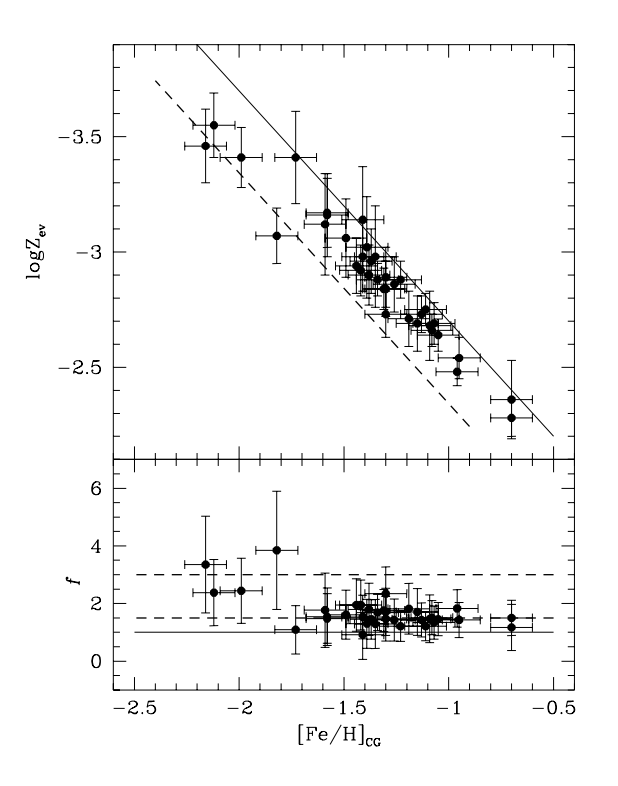


Figure 7. (top) - The evolutionary global metallicity $\log Z_{ev}$ for the GCs in Table 3, as a function of the measured [Fe/H] value (with an uncertainty of \pm 0.10 dex) on the Carretta & Gratton (1997) scale. The solid line represents the canonical correlation for scaled-solar chemical compositions [f=1 in Eq. (1)], while the dashed line refers to f=3. (bottom) - The α -enhancement factor f for the clusters in Table 3 as a function of the measured [Fe/H] value on the Carretta & Gratton (1997) scale. The solid line represents the classical value for scaled-solar chemical compositions (f=1), while the dashed lines denote the average values $f \sim 1.5$ and $f \sim 3$ suggested by clusters with $[\text{Fe/H}] \geq -1.7$ and [Fe/H] < -1.7, respectively.

$$\log Z = -0.154 - 1.330A \tag{7}$$

with $A \geq 2.24$ and A < 2.24, respectively. As shown in the lower panel of Fig. 6, also in this case the discrepancy between the *evolutionary* estimate of the global metallicity (hereafter Z_{ev}) and the original value is close to ± 0.03 dex.

4 GLOBAL METALLICITY FOR GLOBULAR CLUSTERS IN THE GALAXY

In this section we provide accurate *evolutionary* estimates of the global metallicity of a large sample of Galactic GCs, by using the relationships discussed in the previous section.

The sample of Galactic GCs studied in this paper is listed in Table 2. The [Fe/H] values are listed both for the Zinn & West (1984) and the Carretta & Gratton (1997) metallicity scale, while the TO visual magnitudes are from R99, except for the following clusters: NGC 4833 and 5286 (Samus et al. 1995a,b), NGC 5694 (Ortolani & Gratton 1990), NGC 6584 (Sarajedini & Forrester 1995), NGC 6717 (Ortolani et al. 1999), NGC 6934 (Piotto et al. 1999) NGC 7006 (Buonanno et al. 1991) and NGC 7492 (Buonanno et

Table 2. Observed parameters for Galactic Globular Clusters. Iron-to-hydrogen contents are given in the Zinn & West (1984, $[Fe/H]_{ZW}$) and Carretta & Gratton (1997, $[Fe/H]_{CG}$) empirical scales. For the latter scale, the fourth column gives the source: 0 = Carretta & Gratton (1997); 1 = Rutledge, Hesser & Stetson (1997); 2 = Ferraro et al. (2000); 3 = Rosenberg et al. (1999). The $[Fe/H]_{CG}$ value of NGC 7492 has been estimated through the mean relation between $[Fe/H]_{CG}$ and $[Fe/H]_{ZW}$.

NGC	$[\mathrm{Fe}/\mathrm{H}]_{ZW}$	$[\mathrm{Fe}/\mathrm{H}]_{CG}$	Source	V(TO)	V(ZAHB)	V(BUMP)
104	-0.71	-0.70	0	17.60 ± 0.08	14.22 ± 0.07	14.55 ± 0.05
288	-1.40	-1.07	0	18.90 ± 0.04	15.50 ± 0.10	$15.45 {\pm} 0.05$
362	-1.27	-1.15	0	18.79 ± 0.04	15.50 ± 0.07	15.40 ± 0.10
1261	-1.29	-1.08	1,2	19.90 ± 0.06	16.72 ± 0.05	$16.60 {\pm} 0.05$
1851	-1.33	-1.05	1,2	$19.50 {\pm} 0.07$	16.20 ± 0.05	$16.15 {\pm} 0.05$
1904	-1.68	-1.37	0	19.65 ± 0.09	16.27 ± 0.07	15.95 ± 0.05
2808	-1.37	-1.13	1,2	$19.60 {\pm} 0.07$	$16.27 {\pm} 0.07$	$16.15 {\pm} 0.05$
3201	-1.56	-1.23	0	$18.20 {\pm} 0.05$	$14.77 {\pm} 0.07$	$14.55 {\pm} 0.05$
4590	-2.09	-1.99	0	19.05 ± 0.07	15.75 ± 0.05	15.15 ± 0.05
4833	-1.86	-1.58	0	19.20 ± 0.10	15.77 ± 0.07	$15.35 {\pm} 0.05$
5272	-1.66	-1.34	0	19.10 ± 0.04	$15.68 {\pm} 0.05$	$15.45 {\pm} 0.05$
5286	-1.79	-1.49	1,2	20.05 ± 0.10	16.60 ± 0.10	$16.25 {\pm} 0.05$
5694	-1.92	-1.73	1,2	22.12 ± 0.10	18.70 ± 0.10	18.15 ± 0.07
5897	-1.68	-1.59	0	19.75 ± 0.07	$16.45 {\pm} 0.07$	16.00 ± 0.10
5904	-1.40	-1.11	0	18.50 ± 0.03	15.13 ± 0.05	15.00 ± 0.05
6093	-1.68	-1.44	1,2	19.80 ± 0.08	16.12 ± 0.07	15.95 ± 0.10
6121	-1.28	-1.19	0	16.90 ± 0.03	13.45 ± 0.10	13.40 ± 0.10
6171	-0.99	-0.95	1,2	$19.25 {\pm} 0.06$	15.70 ± 0.10	15.85 ± 0.05
6205	-1.65	-1.39	0	18.50 ± 0.06	15.10 ± 0.15	14.75 ± 0.07
6218	-1.61	-1.26	1,2	18.30 ± 0.07	14.75 ± 0.15	14.60 ± 0.07
6229	-1.54	-1.30	2	21.48 ± 0.10	18.11 ± 0.05	18.00 ± 0.07
6254	-1.60	-1.41	0	$18.55 {\pm} 0.05$	$14.85 {\pm} 0.10$	$14.65 {\pm} 0.05$
6341	-2.24	-2.16	0	$18.55 {\pm} 0.06$	15.30 ± 0.10	$14.65 {\pm} 0.05$
6362	-1.08	-0.96	0	18.90 ± 0.08	15.41 ± 0.06	15.60 ± 0.02
6397	-1.91	-1.82	0	16.40 ± 0.04	13.00 ± 0.10	12.60 ± 0.10
6584	-1.54	-1.30	2	20.00 ± 0.10	16.60 ± 0.05	16.40 ± 0.10
6656	-1.75	-1.41	0	17.80 ± 0.07	14.25 ± 0.10	13.90 ± 0.10
6681	-1.51	-1.31	1,2	19.25 ± 0.09	$15.85 {\pm} 0.10$	$15.65 {\pm} 0.05$
6717	-1.32	-1.09	1,2	19.25 ± 0.10	15.75 ± 0.15	15.75 ± 0.10
6752	-1.54	-1.42	0	17.35 ± 0.08	13.90 ± 0.15	$13.65 {\pm} 0.05$
6809	-1.82	-1.58	1,2	17.95 ± 0.12	14.60 ± 0.10	14.15 ± 0.05
6838	-0.58	-0.70	0	17.95 ± 0.06	14.52 ± 0.10	14.80 ± 0.15
6934	-1.54	-1.30	2	20.40 ± 0.15	17.05 ± 0.04	16.78 ± 0.10
7006	-1.59	-1.35	2	22.30 ± 0.10	$18.85 {\pm} 0.15$	$18.55 {\pm} 0.07$
7078	-2.15	-2.12	0	$19.25 {\pm} 0.06$	15.90 ± 0.07	$15.25 {\pm} 0.05$
7492	-1.51	-1.38		21.25 ± 0.10	17.78 ± 0.10	$17.55 {\pm} 0.10$

al. 1987). The ZAHB and RGB-bump observations are from F99, except for the following additional measurements of the RGB-bump level: NGC 6352 and 6397 (Alves & Sarajedini 1999) and NGC 6362 (Piotto et al. 1999). We wish to notice that the two major sets of observations are mutually consistent as the ZAHB visual magnitudes listed by F99 are ~ 0.07 mag fainter than the HB visual magnitudes in R99, except for NGC 6093 and NGC 6254. For these two clusters, the F99 values are brighter than those given by R99 (see later). Moreover, we have also checked that the ZAHB magnitudes given by F99 are consistent with the additional measurements of the TO and RGB-bump visual magnitudes.

As a first step, we determine the values of $A=\Delta V(\text{TO-BUMP})$ -0.566 $\Delta V(\text{TO-ZAHB})$ from the data in Table 2, then we derive the global metallicity using Eq. (4) and Eq. (5). The results for Z_{ev} are listed in column (4) of Table 3, together with the horizontal branch morphological type (HB-type) ‡ from Harris (1996). For the two clusters NGC

6093 and 6254, the last two lines in Table 3 refer to the HB level given by R99.

The correlation between $\log Z_{ev}$ and the measured [Fe/H] parameter[§] is presented in the upper panel of Fig. 7, where the solid line shows the *canonical* correlation $\log Z$ =[Fe/H]-1.7 for scaled-solar chemical compositions. One obtains that almost all the clusters present a mild overabundance of the global metallicity with respect to the measured iron-to-hydrogen content. In terms of α -element enhancement [see Eq. (1)], we show in the bottom panel in Fig. 7 that the clusters with [Fe/H] \geq -1.7 show $f \sim$ 1.5, whereas the four most metal-poor clusters show $f \sim$ 3 (dashed lines).

Figure 8 displays the results based on Vdb computations. These models suggest slightly larger Z_{ev} values (see data listed in column (5) of Table 3) in comparison with our models, with an average difference of 0.08 ± 0.06 dex which is within the uncertainty of the derived global metallicity.

[‡] The HB-type is given by the ratio (B-R)/(B+V+R), where B and R denote the number of HB stars blueward and redward of

the RR Lyrae instability strip, respectively, and V is the number of RR Lyrae stars.

 $[\]S$ Note that the measured [Fe/H] values are taken with an uncertainty of ± 0.10 dex.

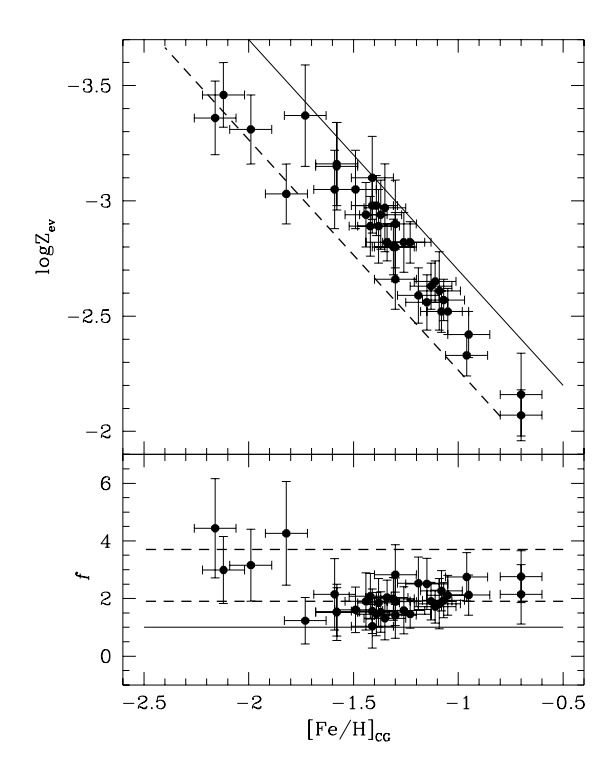


Figure 8. As in Fig. 7, but for Vdb models. The dashed line in the top panel refers to f=3.7, while the dashed lines in the bottom panel denote the average values $f \sim 1.9$ and $f \sim 3.7$ suggested by clusters with $[\text{Fe/H}] \geq -1.7$ and [Fe/H] < -1.7, respectively.

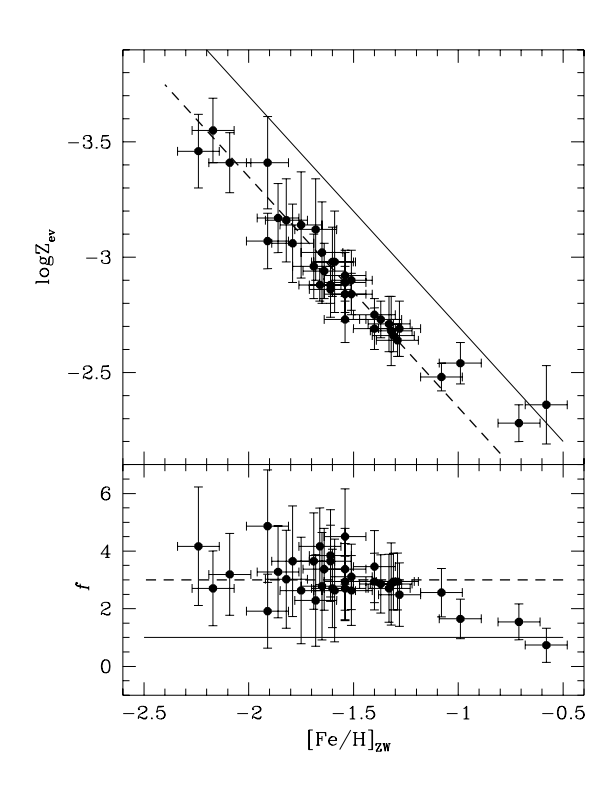


Figure 9. As in Fig. 7, but for the [Fe/H] scale by Zinn & West (1984). The dashed line in both panels refer to an α -enhancement factor $f \sim 3$ suggested by clusters with [Fe/H] ≤ -1.3 .

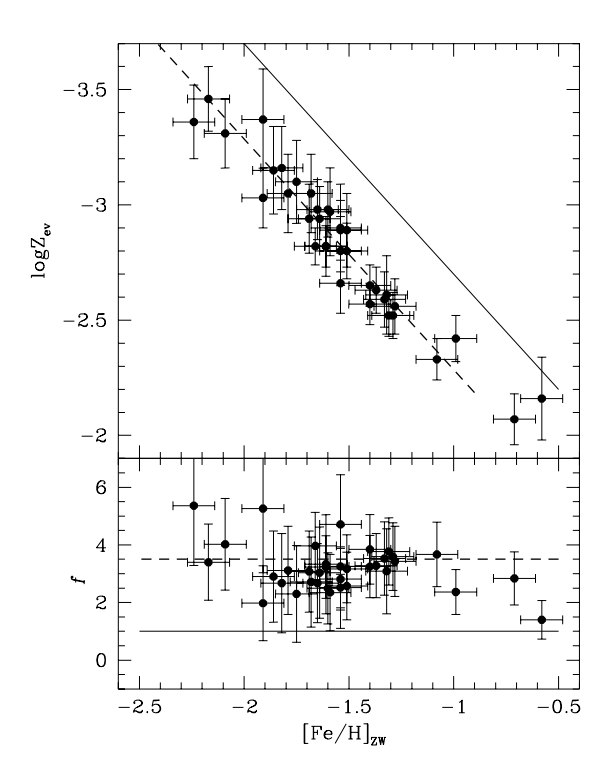


Figure 10. As in Fig. 9, but for Vdb models. The dashed line in both panels refers to an α -enhancement factor $f \sim 3.5$ suggested by clusters with [Fe/H] ≤ -1.3

Also the α -element enhancement is slightly increased, clusters with [Fe/H] ≥ -1.7 now showing $f \sim 1.9$, whereas the four most metal-poor clusters show $f \sim 3.7$ (dashed lines).

We remark here that the global metallicity given in Table 3 are derived from the differential parameters $\Delta V(\text{TO-ZAHB})$ and $\Delta V(\text{TO-BUMP})$ and are fully independent of the measured iron-to-hydrogen content. On the contrary, the f enhancement factors plotted in the lower panel of Figs. 7 and 8 obviously depend on the adopted empirical [Fe/H] scale. When we consider the Zinn & West (1984) scale the results are quite different. As shown in Fig. 9 and Fig. 10, the α -enhancement factor is $f \sim 3$ (our models) or ~ 3.5 (Vdb models) with [Fe/H] ≤ -1.3 , declining toward the solar value $f \sim 1$ at larger metallicities.

The abundances of α –elements in Population II stars provide fundamental constraints to the chemical evolution models of the Galaxy. Several spectroscopic studies have been devoted to this problem (see Carretta, Gratton & Sneden 2000 for discussion and references). As a whole, α –elements appear to be overabundant by a constant factor \sim 2-3 in metal-poor stars, declining toward scaled solar ratios around [Fe/H]=-1.0. As the run of $[\alpha/\text{Fe}]^{\P}$ with [Fe/H] is required to study the chronology of the Galactic halo formation (Matteucci & Francois 1992), we notice that mild variations of the empirical [Fe/H] scale may lead to quite different pictures for the dependence of $[\alpha/\text{Fe}]$ on [Fe/H], and different [Fe/H] values for the transition toward scaled-solar ratios.

¶ $[\alpha/\text{Fe}] = \log f$.

Table 3. Global metallicity for our selected sample of Galactic GCs.

NGC	$[\mathrm{Fe/H}]_{CG}$	НВ	$\log Z_{ev}$	$\log Z_{ev}(\mathrm{Vdb})$
104	-0.70	-0.99	-2.28 ± 0.08	-2.07 ± 0.11
288	-1.07	+0.98	-2.69 ± 0.09	-2.57 ± 0.09
362	-1.15	-0.87	-2.69 ± 0.12	-2.56 ± 0.12
1261	-1.08	-0.71	-2.66 ± 0.07	-2.52 ± 0.09
1851	-1.05	-0.36	-2.64 ± 0.07	-2.52 ± 0.10
1904	-1.37	+0.89	-2.96 ± 0.14	-2.94 ± 0.15
2808	-1.13	-0.49	-2.73 ± 0.08	-2.63 ± 0.10
3201	-1.23	+0.08	-2.88 ± 0.08	-2.82 ± 0.09
4590	-1.99	+0.44	-3.41 ± 0.13	-3.31 ± 0.15
4833	-1.58	+0.93	-3.17 ± 0.15	-3.15 ± 0.17
5272	-1.34	+0.08	-2.88 ± 0.07	-2.82 ± 0.08
5286	-1.49	+0.80	-3.06 ± 0.17	-3.05 ± 0.18
5694	-1.73	+1.00	-3.41 ± 0.20	-3.37 ± 0.22
5897	-1.59	+0.86	-3.12 ± 0.22	-3.05 ± 0.18
5904	-1.11	+0.31	-2.75 ± 0.07	-2.65 ± 0.09
6093	-1.44	+0.93	-2.94 ± 0.12	-2.94 ± 0.14
6121	-1.19	-0.06	-2.71 ± 0.12	-2.59 ± 0.12
6171	-0.95	-0.73	-2.54 ± 0.09	-2.42 ± 0.10
6205	-1.39	+0.97	-3.02 ± 0.22	-2.98 ± 0.13
6218	-1.26	+0.97	-2.86 ± 0.12	-2.82 ± 0.13
6229	-1.30	+0.24	-2.73 ± 0.10	-2.66 ± 0.13
6254	-1.41	+0.98	-2.98 ± 0.15	-2.98 ± 0.12
6341	-2.16	+0.91	-3.46 ± 0.16	-3.36 ± 0.16
6362	-0.96	-0.58	-2.48 ± 0.06	-2.33 ± 0.09
6397	-1.82	+0.98	-3.07 ± 0.12	-3.03 ± 0.13
6584	-1.30	-0.15	-2.84 ± 0.12	-2.80 ± 0.15
6656	-1.41	+0.92	-3.14 ± 0.23	-3.10 ± 0.18
6681	-1.31	+0.96	-2.84 ± 0.09	-2.80 ± 0.12
6717	-1.09	+0.98	-2.68 ± 0.15	-2.61 ± 0.18
6752	-1.42	+1.00	-2.92 ± 0.11	-2.89 ± 0.13
6809	-1.58	+0.87	-3.16 ± 0.18	-3.16 ± 0.19
6838	-0.70	-1.00	-2.36 ± 0.17	-2.16 ± 0.18
6934	-1.30	+0.25	-2.89 ± 0.13	-2.90 ± 0.18
7006	-1.35	-0.28	-2.98 ± 0.22	-2.97 ± 0.19
7078	-2.12	+0.67	-3.55 ± 0.14	-3.46 ± 0.14
7492	-1.38	+0.81	-2.90 ± 0.13	-2.89 ± 0.17
6093	-1.44	+0.93	-3.12 ± 0.22	-2.97 ± 0.15
6254	-1.41	+0.98	-3.27 ± 0.15	-3.23 ± 0.16

Both the distribution and absolute values of the α -element enhancement suggested by our method together with the Zinn & West (1984) [Fe/H] scale appear in fine agreement with the empirical results by Carney (1996). On the contrary, the results obtained using the Carretta & Gratton (1997) [Fe/H] scale do not appear fully supported by current spectroscopic measurements. Even though to investigate the accuracy of current empirical [Fe/H] scales is out of the aim of the present paper, we wish to emphasize that this is still a controversial issue. We also wish to notice that recently Vandenberg (2000) and Bergbusch & Vandenberg (2001) have provided some additional evidence, based on the comparison between their theoretical isochrones and CMDs of Galactic GCs, that the metallicities determined by Carretta & Gratton (1997), mainly for the intermediatemetallicity clusters, are too high, values close to the Zinn & West (1984) scale being more favourite. Present analysis provides independent support to their claim.

Before closing this section, it is worthwhile to emphasize that our method, being based only on well defined observational features of the CMD, appears quite suitable for deriving accurate estimates of the GC global metallicity. It uses only differential quantities, i.e. visual magnitude differences,

and its results are therefore insensitive to uncertainties on the zero point of the CMD photometric calibration as well as on the cluster distance and reddening.

It is also worth noticing that the method relies on observables whose properties are not significantly affected by non-canonical processes occurring along the RGB, like deepmixing processes, which are currently invoked to explain the chemical abundance patterns observed in RGB stars of many Galactic GCs (Sweigart & Mengel 1979, Langer, Hoffman & Sneden 1993). As suggested by theoretical predictions (Mestel 1957) and spectroscopic data (Charbonnel, Brown, & Wallerstein 1998, and references therein), molecular weight gradients, such as the H-discontinuity left over in the envelope of RGB stars by the first dredge up, should be able to inhibit these non-canonical mixing processes, which are therefore expected to be efficient only after the RGB bump.

5 SUMMARY

The main results obtained in present work can be summarized as follows:

- We have developed an homogeneous theoretical scenario, based on updated stellar models including atomic diffusion, computed for a wide metallicity range; this allows us to predict the behaviour with the cluster metallicity and age of relevant observational features of the CM diagram, such as the Turn Off magnitude and the brightness of both the ZAHB at the level of the RR Lyrae instability strip, and the RGB-bump;
- we define a new observable based on the visual magnitude difference between the TO and the ZAHB ΔM_V (TOZAHB), and the TO and the RGB-bump ΔM_V (TOBUMP), namely, $A = \Delta M_V$ (TO-BUMP) $-0.566\Delta M_V$ (TOZAHB). We show that the parameter A does not depend at all on the cluster age, whereas it does strongly correlate with the global cluster metallicity. The calibration of the parameter A as a function of Z is provided;
- by using this calibration, together with a large observational database of Galactic GCs, we estimate the global metallicity of a large sample of GCs. Our estimates are independent of empirical metallicity measurements, but strongly rely on the accuracy and reliability of the adopted theoretical models. By using our global metallicity determinations, together with presently available [Fe/H] determinations (Zinn & West 1984 or Carretta & Gratton 1997), and using the relation provided by Salaris et al. (1993) that connects global metallicity to [Fe/H] and α -element enhancement, we are able to provide an estimate of the [α /Fe] ratio for the individual clusters in our sample;
- the trend of $[\alpha/\text{Fe}]$ with [Fe/H] we predict when using the Zinn & West metallicity scale, appears in fine agreement with current spectroscopical measurements, which suggest a rather constant overabundance of α -elements in metalpoor stars, and a decline toward the solar ratios around $[\text{Fe}/\text{H}] \approx -1.0$. This picture is not supported when we use the Carretta & Gratton [Fe/H] scale;
- the calibration of the $A-Z_{ev}$ relation is model dependent, in the sense that the Vdb models, which are based on different input physics, yields a slightly different formulation of the parameter A, given by $A=\Delta M_V$ (TO-BUMP)-0.487 ΔM_V (TO-ZAHB). However, the resulting

 Z_{ev} values are only 0.08 ± 0.06 dex larger than the results based on our computations;

- the good agreement between the global metallicity estimates provided by our models accounting for atomic diffusion, and the ones obtained by employing Vdb models which neglect atomic diffusion, shows that the theoretical calibration of the A parameter is only marginally affected by the efficiency of this non-canonical process;
- the present analysis clearly demonstrates that the our newly defined observational parameter, independent of the uncertainty on the zero point of the photometric calibration as well as on the cluster distance and reddening, is a powerful indicator of globular cluster global metal abundances.

Acknowledgments:

We warmly thank D. Vandenberg, P. Bergbusch and M. Salaris for sending us data about their theoretical models. We gratefully also acknowledge M. Salaris for an accurate reading of an early version of this manuscript and for his helpful comments. We thank the anonymous referee for several helpful suggestions and comments. One of us (C.S.) wishes to acknowledge the Max Planck Institut für Astrophysik for the kind hospitality during the early phase of this work. Financial support for this work was provided by MIUR-COFIN2000, under the scientific project "Stellar observables of cosmological relevance".

REFERENCES

Alexander, D.R., Ferguson, J.W., 1994, ApJ, 437, 879

Alves, D.R., Sarajedini, A., 1999, ApJ, 511, 225

Basu, S., Pinsonneault, M.H., Bahcall, J.N., 2000, ApJ, 529, 1084 Bergbusch, P.A., Vandenberg, D.A., 2001, ApJ, 556, 322

Buonanno, R., Corsi, C.E., Ferraro, I., Fusi Pecci, F., 1987, A&AS, 67, 327

Buonanno, R., Fusi Pecci, F., Capellaro, E., Ortolani, S., Richtler, T., Geyer, E.H., 1991, AJ, 102, 1005

Carney, B. W., 1996, PASP, 108, 900

Carretta E., Gratton R.G., 1997, A&AS, 121, 95

Carretta E., Gratton R.G., Sneden, C., 2000, A&A, 356, 238

Cassisi S., Castellani V., Degl'Innocenti S., Salaris M., Weiss A., 1999, A&AS, 134, 103

Cassisi S., Castellani V., Degl'Innocenti S., Weiss A., 1998, A&AS, 129, 267

Cassisi, S., Salaris, M., 1997, MNRAS, 285, 593

Castellani, V., Chieffi, A., Tornambé, A., Pulone, L., 1985, ApJ, 296, 204

Castellani, V., Ciacio, F., Degl'Innocenti, S., Fiorentini, S., 1997, A&A, 322, 801

Castelli F., Gratton R.G., Kurucz R.L., 1997a, A&A, 318, 841

Castelli F., Gratton R.G., Kurucz R.L., 1997b, A&A, 324, 432

Castilho, B.V., Pasquini, L., Allen, D.M., Barbuy, B., Molaro, P., 2000, A&A, 361, 92

Charbonnel, C., Brown, J. A., Wallerstein, G., 1998, A&A, 332, 204

Chieffi, A., Straniero, O. 1989, ApJS, 71, 47

Ferraro, F. R., Messineo, M., Fusi Pecci, F., de Palo, M. A., Straniero, O., Chieffi, A., Limongi, M. 1999, AJ, 118, 1738

Frogel, J.A., Persson, S.E., & Cohen, J.G. 1983, ApJS, 53, 713

Fusi Pecci, F., Ferraro, F.R., Crocker, D.A., Rood, R.T., Buonanno, R. 1990, A&A, 238, 95

Gratton, R. G., et al. 2001, A&A, 369, 87

Harris, W.E., 1996, AJ, 112, 1487

Iben, I. Jr., 1968, Nature, 220, 143

Iglesias, C.A., Rogers, F.J., Wilson, B.G., 1992, ApJ, 397, 717

Itoh, N., Mitake, S., Iyetomi, H., Ichimaru, S. 1983, ApJ, 273, 774 King, C.R., Da Costa, G.S., Demarque, P., 1985, ApJ, 299, 674

Langer, G.E., Hoffman, R., Sneden, C., 1993, PASP, 105, 301 Matteucci, F., Francois, P., 1992, A&A, 262, L1

Mestel, L. 1957, ApJ, 126, 550

Ortolani, S., Barbuy, B., Bica, E., 1999, A&AS, 136, 237

Ortolani, S., Gratton, R.G., 1990, A&AS, 82, 71

Piotto, G., Zoccali, M., King, I.R., Djorgovski, S.G., Sosin, C., Dorman, B., Rich, R.M., Meylan, G., 1999, AJ, 117, 264

Ramírez, S.V., Cohen, J.G., Buss, J., Briley, M.M., 2001, AJ, 122, 1429

Rogers, F.J., Swenson, F.J., & Iglesias, C.A., 1996, ApJ, 456, 902
 Rosenberg, A., Saviane, I., Piotto, G., Aparicio, A., 1999, AJ, 118, 2306

Ross, J.E., Aller, L.H. 1976, Science, 1991, 1223

Rutledge, G.A., Hesser, J.E., Stetson, P. B., 1997, PASP, 109, 907

Salaris, M., Chieffi, A., Straniero, O. 1993, ApJ, 414, 580

Salaris, M., Weiss, A., 1997, A&A, 327, 107

Salaris, M., Weiss, A., 1998, A&A, 335, 943

Samus, N., Kravtsov, V., Pavlov, M., Alcaino, G., Liller, W., 1995a, A&AS, 109, 479

Samus, N., Ipatov, A., Smirnov, O., Kravtsov, V., Alcaino, G., Liller, W., Alvarado, F., 1995b, A&AS, 112, 439

Sarajedini, A., Chaboyer, B., Demarque, P., 1997, PASP, 109, 1321

Stetson, P.B., Vandenberg, D.A., Bolte, M., 1996, PASP, 108, 560 Straniero, O., 1988, A&AS, 76, 157

Straniero, O., 1988, A&AS, 70, 157

Straniero, O., Chieffi, A., Limongi, M., 1997, ApJ, 490, 425

Sweigart, A.V., Mengel, J.G., 1979, ApJ, 229, 624

Thomas, H.C., 1967, Z. Astroph., 67, 420

Thoul, A.A., Bahcall, J.N., Loeb, A., 1994, ApJ, 421, 828

Vandenberg, D.A., 2000, ApJS, 129, 315

VandenBerg, D.A., Swenson, F.J., Rogers, F.J., Iglesias, C.A., Alexander, D.R., 2000, ApJ, 532, 430

Yi, S., Demarque, P., Lee, Y-.W., Ree, C., Lejeune, T., Barnes, S., 2001, ApJS, 136, 417

Zinn, R., 1985, ApJ, 293, 424

Zinn, R., West, M.J., 1984, ApJS, 55, 45

Zoccali, M., Cassisi, S., Bono, G., Piotto, G., Rich, R. M., Djorgovski, S. G., 2000, ApJ, 538, 289